

Renzo L. Ricca* and Francesca Maggioni

Groundstate energy spectra of knots and links: magnetic versus bending energy

Abstract: In this paper we review recent results on the groundstate energy spectra of magnetic knots and links and compare these results with new results on bending energy of tight knots and links obtained by using RIDGERUNNER data on curvature. Remarkable similarities between the two systems are found. Comparative analysis between magnetic and bending energy at groundstate energy level shows that information based on bending energy provides a very good proxy for magnetic end-states.

Keywords: Knots, links, energy spectrum, constrained minimization, magnetic relaxation, bending energy, topological fluid mechanics.

MSC: 57M25, 76M30, 76B47, 76W99

13.1 Introduction


In recent years much progress has been done in applications of knot theory to mathematical physics, from classical to quantum field theory, and in physical and biological sciences as well. This has led mathematical research to explore new territories at the cross-road of several, different disciplines. One interesting problem here is the study of minimum energy states of physical knots and links subject to continuous relaxation (through diffeomorphisms) of some energy functional. Magnetic relaxation of knots and links embedded in an ideal fluid provides indeed a prototype example of minimization useful to explore and understand similar features present, for instance, in elastic systems. Here we present a brief review of results on the groundstate energy spectra of magnetic knots and links (published in *J. Phys. A: Math. & Theor.* [20]) that sheds light on similar aspects when we consider elastic, rather than magnetic knots and links. Indeed proof of how good this analogy can be is given by comparing, as we do here, those results with new results based on bending energy estimates of tight knots and links obtained by using data readily available from RIDGERUNNER [1].

The material is presented as follows. In Sec. 13.2 we consider magnetic knots and links as tubular embeddings in ideal magnetohydrodynamics and introduce basic definitions. The prototype problem of magnetic relaxation under constraints is discussed in Sec. 13.3. A solution to the problem of magnetic relaxation of (zero-framed) knots

*Corresponding author: **Renzo L. Ricca**, Department of Mathematics and Applications, U. Milano-Bicocca, Via Cozzi 55, 20125 Milano, Italy & Beijing–Dublin International College, Beijing U. Technology, 100 Pingleyuan, Beijing 100124, PR China, E-mail: renzo.ricca@unimib.it

Francesca Maggioni, Department of Management, Economics & Quantitative Methods, U. Bergamo, Via dei Caniana 2, 24127 Bergamo, Italy, E-mail: francesca.maggioni@unibg.it

<https://doi.org/10.1515/9783110571493-012>

Open Access.  © 2018 Renzo L. Ricca and Francesca Maggioni, published by De Gruyter. This work is licensed under the Creative Commons Attribution-NonCommercial-NoDerivs 4.0 License.

Brought to you by | Università degli Studi di Bergamo

Authenticated

Download Date | 11/4/19 9:59 AM

and links is presented in Sec. 13.4. By using RIDGERUNNER data the groundstate magnetic energy spectra of the first 250 prime knots and 130 prime links are presented (Sec. 13.5). Similar spectra for the bending energy of tight knots and links are presented in Sec. 13.6. A comparative analysis of these results is made in Sec. 13.7. Finally, conclusions are drawn in Sec. 13.8.

13.2 Magnetic knots and links in ideal conditions

We consider magnetic knots and links in an ideal, incompressible, perfectly conducting fluid in S^3 (i.e. $\mathbb{R}^3 \cup \{\infty\}$, simply connected). Let $\mathbf{u} = \mathbf{u}(\mathbf{x}, t)$ be the fluid velocity, smooth function of the position vector \mathbf{x} and time t , with $\nabla \cdot \mathbf{u} = 0$ in S^3 and $\mathbf{u} = 0$ at infinity. The magnetic field $\mathbf{B} = \mathbf{B}(\mathbf{x}, t)$ is frozen in the fluid and has finite energy, that is

$$\mathbf{B} \in \{\nabla \cdot \mathbf{B} = 0, \partial_t \mathbf{B} = \nabla \times (\mathbf{u} \times \mathbf{B}), L_2\text{-norm}\}. \quad (13.2.1)$$

A magnetic knot is a magnetic flux tube prescribed by the knot type \mathcal{K} and the magnetic field \mathbf{B} , defined on a *regular* tubular support $\mathcal{T}(\mathcal{K})$ centered on \mathcal{K} . We assume \mathcal{K} to be a C^3 -smooth, closed loop (i.e. a submanifold of S^3 homeomorphic to S^1), simple (i.e. non-self-intersecting) and parametrized by arc-length s . The tube $\mathcal{T} = \mathcal{K} \otimes \mathcal{S}$, given by the cartesian product of \mathcal{K} and the circular disk \mathcal{S} , is centered on the knot, whose total length is $L = L(\mathcal{K})$ (hence $s \in [0, L]$), local radius of curvature $\rho > 0$, and cross-sectional area $A = \pi R^2$ of radius $R > 0$.

Since the magnetic knot is a physical tube, it is useful to introduce the volume $V(\mathcal{T})$, the magnetic flux Φ and the magnetic energy M . The total volume is given by $V = V(\mathcal{T}) = \pi R^2 L$, with tubular boundary $\partial\mathcal{T}$ a magnetic surface, i.e.

$$\text{supp}(\mathbf{B}) := \mathcal{T}(\mathcal{K}), \quad \mathbf{B} \cdot \hat{\nu}_\perp = 0 \text{ on } \partial\mathcal{T}, \quad (13.2.2)$$

where $\hat{\nu}_\perp$ is a unit normal to $\partial\mathcal{T}$. The existence and regularity of non-self-intersecting nested tori, support of the magnetic field inside \mathcal{T} , is guaranteed by the tubular neighborhood theorem [22], provided $\rho \geq R$ all along \mathcal{K} . The magnetic flux Φ is defined by

$$\Phi = \int_{\mathcal{S}} \mathbf{B} \cdot \hat{\nu} \, d^2 \mathbf{x}, \quad (13.2.3)$$

where now $\hat{\nu}$ is the unit normal to \mathcal{S} ; the magnetic energy M is given by

$$M = \frac{1}{2} \int_{V(\mathcal{T})} \|\mathbf{B}\|^2 \, d^3 \mathbf{x}. \quad (13.2.4)$$

13.3 The prototype problem

For a magnetic knot, whose field is confined to a single tube of *signature* (V, Φ) , the combined action of magnetic stresses and Lorentz force induces the field lines to shrink like elastic bands, by shortening the knot, while conserving volume and flux [12]. Magnetic energy gets gradually converted into kinetic energy, and eventually dissipated by viscosity or other dissipative effects, if present. As the relaxation progresses, the average cross-section increases proportionately, and the tubular knot becomes thicker and tighter, until knot topology prevents any further adjustment: the final state is ultimately reached when the relaxation comes to a complete stop (see figure 13.1). During this process the knot is also gradually deformed by the action of a signature-preserving flow (through diffeomorphisms), that governs the relaxation from the initial configuration. Since the tight configuration of the end-state resembles that of an *ideal* knot of platonic features [23], magnetic relaxation provides physical mechanism to investigate optimal geometric properties of ideal knots.

Let (r, ϑ_R, s) denote an *orthogonal*, curvilinear coordinate system centered on \mathcal{K} (see [11]); $r \in [0, R]$ and $\vartheta_R \in [0, 2\pi]$ are the radial and azimuthal coordinates in the cross-sectional plane of \mathcal{S} , with origin O at $s = 0$ and $\vartheta_R = 0$ given by the direction of the principal normal to \mathcal{K} at O . The metric is orthogonal, with scale factors $h_r = 1$, $h_{\vartheta_R} = r^2$, $h_s = 1 - cr \cos \vartheta$, where $c = c(s)$ is curvature,

$$\vartheta = \vartheta(\vartheta_R, s) = \vartheta_R - \int_0^s \tau(\bar{s}) d\bar{s}, \quad (13.3.1)$$

and $\tau = \tau(s)$ torsion. Orthogonality is ensured by eq. (13.3.1), which provides the necessary correction to the standard azimuthal angle by the torsion contribution (see details in [11], Sec. 3). The results presented here are derived by using this metric.

The magnetic field \mathbf{B} may be decomposed into meridian and longitudinal components, that is

$$\mathbf{B} = (0, B_{\vartheta_R}(r), B_s(r)), \quad (13.3.2)$$

and in general we assume that the longitudinal field is far greater than the meridian field, i.e. $B_s \gg B_{\vartheta_R}$. This is consistent with the usual definition of twisted flux tube, whose field lines wind around the knot axis in the longitudinal direction. By using the solenoidal condition $\nabla \cdot \mathbf{B} = 0$, the magnetic field can be expressed in terms of poloidal (meridian) and toroidal (longitudinal) fluxes Φ_P and Φ_T , i.e.

$$\mathbf{B} = \left(0, \frac{1}{L} \frac{d\Phi_P}{dr}, \frac{1}{2\pi r} \frac{d\Phi_T}{dr} \right) + \left(0, \frac{\partial \tilde{\psi}}{\partial s}, -\frac{\partial \tilde{\psi}}{\partial \vartheta_R} \right), \quad (13.3.3)$$

where the total field is given by the sum of an average field plus a fluctuating field with zero net flux, in terms of the flux function $\tilde{\psi} = \tilde{\psi}(r, \vartheta_R, s)$. The twist $h = \Phi_P / \Phi_T$ of the



Fig. 13.1: Ideal relaxation of a magnetic trefoil knot and a Hopf link.

field lines provides the magnetic field *framing* given by $(2\pi)^{-1}$ times the turns of twist required to generate poloidal field from toroidal field, starting from $\Phi_p = 0$.

According to the process described above, knot topology dictates a lower bound on the relaxation of magnetic energy M , which must be bounded from below by a minimum $M_{\min} > 0$, that on dimensional grounds is given by (see [13])

$$M_{\min} = m(h)\Phi^2 V^{-1/3}, \tag{13.3.4}$$

where $m(h)$ is a positive, dimensionless function of the internal twist h . Of particular interest is the value of h for which $m(h)$ is minimal (m_{\min}). A fundamental problem is this:

Problem 1 ([14]). Determine m_{\min} for knots of minimum crossing number 3, 4, 5, ...

If c_{\min} denotes the *topological crossing number* of the knot and $h = 0$ (a condition referred to as *zero-framing*), one can prove the following result:

Theorem 1 ([16]). Let \mathcal{K} be a zero-framed magnetic knot with signature $\{V, \Phi\}$. We have $m(0) = (2/\pi)^{1/3} c_{\min}$; hence

$$M_{\min} = \left(\frac{2}{\pi}\right)^{1/3} c_{\min} \Phi^2 V^{-1/3}. \tag{13.3.5}$$

For a signature-preserving flow, eq. (13.3.5) establishes a correspondence between minimum energy levels and topology. However, $M_{\min} \propto c_{\min}$ is a rather loose result. From a direct inspection of the knot table (see, for instance, the standard tabulation in [21]) with the exception of the trefoil and the 4-crossing knot, for all other values of $c_{\min} > 4$ there are several distinct knot types for each given c_{\min} , and the number gets exponentially large for increasing values of c_{\min} (2 for $c_{\min} = 5$, 3 for $c_{\min} = 6$, 7 for $c_{\min} = 7$, 21 for $c_{\min} = 8$, and so on). Hence, the question is to determine whether a one-to-one relationship between energy minima and different knot types of same c_{\min} may exist or not.

13.4 Relaxation of magnetic knots and constrained minima

To explore this problem let us consider the relaxation of a magnetic flux tube in some generality. Let $V_r = \pi r^2 L$ be the partial volume of the tubular neighborhood of radius r ; the ratio of the partial to total volume is given by $V_r/V(\mathcal{J}) = (r/R)^2$. Now, let $f(r/R)$ be a monotonically increasing function of r/R ; for example $f(r/R) = (r/R)^\gamma$, with $\gamma > 0$; $\gamma = 2$ defines the *standard* flux tube. A detailed analysis of the relaxation of magnetic flux tube with twist is done in [11]. By using the orthogonal, curvilinear system (r, ϑ_R, s) and the magnetic field decomposition given by (13.3.3), standard minimization of (13.2.4) is carried out and under the periodicity of ϑ_R and s , subject to these assumptions:

- (i) $\{V, \Phi\}$ is invariant;
- (ii) the circular cross-section is independent of s ;
- (iii) $\tilde{\psi}$ is independent of s ;
- (iv) the knot length is independent of h .

We have:

Theorem 2 ([11]). Let \mathcal{K} be an essential magnetic knot with signature $\{V, \Phi\}$ and magnetic field given by (13.3.3). Constrained minimization of magnetic energy yields

$$M^* = \left(\frac{\gamma^2 L^{*2}}{8(\gamma - 1)V} + \frac{\gamma \pi h^2}{2L^*} \right) \Phi^2, \tag{13.4.1}$$

where L^* is the minimal tube length of the tight knot.

For a standard flux tube ($\gamma = 2$), (13.4.1) reduces to

$$M^* = \left(\frac{L^{*2}}{2V} + \frac{\pi h^2}{L^*} \right) \Phi^2. \tag{13.4.2}$$

This result is equivalent to the eq. (4.2) of [7] (coefficients left undetermined). Note that because of the constraints, for any given knot family we have that $\langle M^* \rangle_{c_{\min}} \geq M_{\min}$, where angular brackets denote averaging over the number of knots of the same c_{\min} family.

In order to investigate the relation between energy and knot topology, let us refer to standard flux tubes; it is useful to rewrite eq. (13.4.2) in terms of *ropelength*, a useful measure of knot complexity [4]: this is defined by $\lambda = L^*/R^*$, where L^* is the minimal length and R^* the maximal cross-sectional radius of the knot in tight configuration. In the case of the unknot, the least possible value of λ (say λ_0) is that given by the tight torus; hence $\lambda \geq \lambda_0 = 2\pi$. By using $V = \pi R^{*2} L^* = \text{cst.}$, and after some straightforward algebra, we have

$$M^* = \left(\frac{\lambda^{4/3}}{2\pi^{2/3}} + \frac{\pi^{4/3} h^2}{\lambda^{2/3}} \right) \Phi^2 V^{-1/3}. \tag{13.4.3}$$

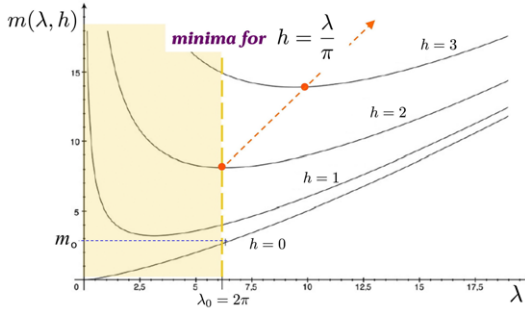


Fig. 13.2: Influence of twist h on the energy function $m(\lambda, h)$, plotted against ropelength λ , according to eq. (13.4.4). The absolute minimum is given by the tight torus, for which $\lambda = \lambda_0 = 2\pi$ and $m_0 \approx 2.70$ (from [20]).

By comparing (13.3.4) and (13.4.3), and under the above assumptions, we can state that

$$m(\lambda, h) = \frac{\lambda^{4/3}}{2\pi^{2/3}} + \frac{\pi^{4/3} h^2}{\lambda^{2/3}}, \tag{13.4.4}$$

showing the explicit dependence of minimum energy on ropelength and framing

13.5 Groundstate magnetic energy spectra

Let us first investigate the minima $m_{\min} = m_{\min}(h)$ by plotting (13.4.4) against λ for $h = 0, 1, 2, 3, \dots$ (see figure 13.2). The absolute minimum m_0 corresponds to the zero-framed unknot (tight torus), given by $h = 0$ and $\lambda = \lambda_0 = 2\pi$: $m_0 = (2\pi^2)^{1/3} \approx 2.70$. The groundstate energy of zero-framed flux tubes provides the absolute minimum energy level; $m(h)$ remains a monotonic increasing function of λ for $h \leq 2$: at $\lambda_0 = 2\pi$ we have $m(h = 1) = 4.05$ and $m(h = 2) = 8.11$. For $h \geq 2$ the energy minima are attained at $h = \lambda/\pi$; thus, by substituting the optimal value $\lambda = \pi h$ in (13.4.4), we have

$$m_{\min}(h) = \frac{3}{2} \pi^{2/3} h^{4/3} \quad (h \geq 2). \tag{13.5.1}$$

For $h > 2$ (and $\lambda \geq \lambda_0$) the functional dependence of $m(h)$ on λ ceases to be monotonic. The same $h^{4/3}$ power-law of eq. (13.5.1) was also found by [7] (p. 206, eq. 4.15, by scaling arguments).

The minimum energy spectra of the first prime knots and links is determined by setting $h = 0$ in (13.4.4) and by using ropelength data (λ_K) of each knot/link type K obtained by RIDGERUNNER, a tightening algorithm developed by [1]. A particularly simple expression is obtained by normalizing $m(\lambda_K, 0)$ with respect to the minimum energy

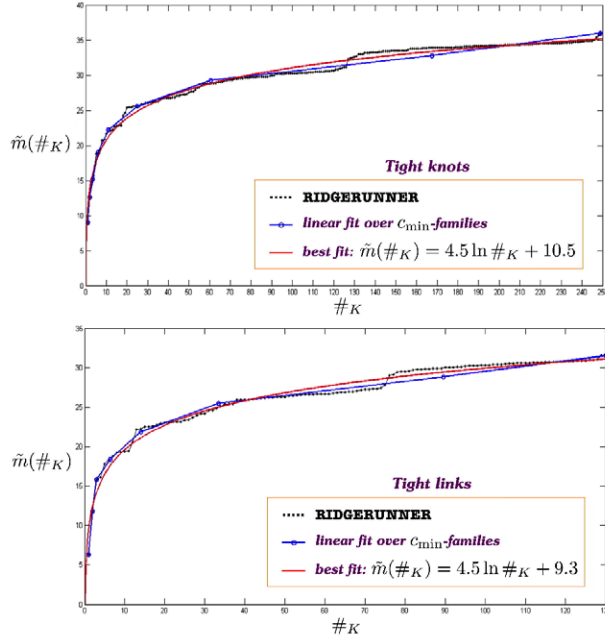


Fig. 13.3: Magnetic energy spectrum $\tilde{m} = \tilde{m}(\#_K)$ of tight knots (top) and tight links (bottom) plotted against the knot/link number $\#_K$, given by the position of the knot/link K listed according to increasing value of ropelength $\lambda_K = \lambda(\#_K)$ (from [20]).

value m_o of the tight torus; thus, we have

$$\tilde{m}(K) = \frac{m(\lambda_K, 0)}{m_o} = \left(\frac{\lambda_K}{2\pi} \right)^{4/3}, \tag{13.5.2}$$

that gives a one-to-one relationship between minimum energy level and knot ropelength. Since the relation $\lambda_K = \lambda(K)$ is not known analytically, it must be reconstructed from numerical data. We take $\lambda_K = \lambda(\#_K)$, where $\#_K$ denotes the position of the knot/link K listed according to increasing values of ropelength given by RIDGERUNNER. Hence, instead of tabulating energy levels as function of the knot/link position given by standard knot tabulation, by taking $\lambda_K = \lambda(\#_K)$ we plot $\tilde{m} = \tilde{m}(\#_K)$, according to increasing ropelength data. The energy spectra are shown in figure 13.3 for the first 250 prime knots up to 10 crossings (top diagram) and 130 prime links up to 9 crossings (bottom diagram). Remarkably, magnetic energy levels of knot and link types seem to follow an almost identical logarithmic law given by the best fit curve shown in the plots.

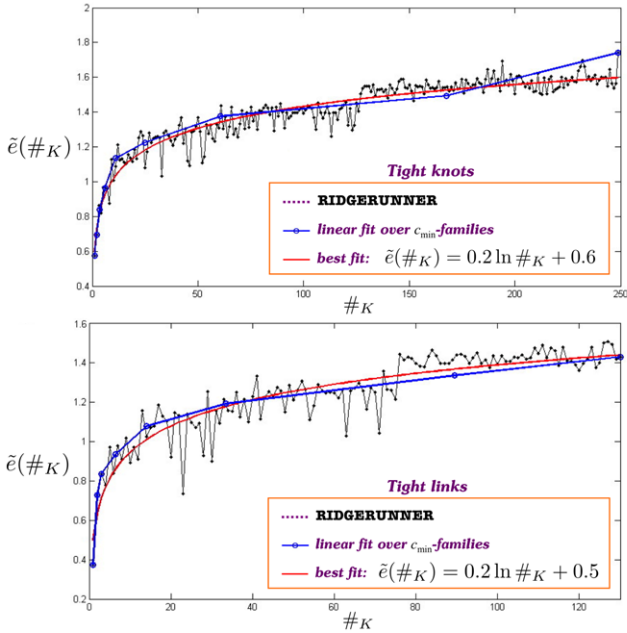


Fig. 13.4: Bending energy spectrum $\tilde{e} = \tilde{e}(\#K)$ of tight knots (top) and links (bottom) plotted against the knot/link number $\#K$, given by the position of the knot/link K listed according to increasing values of ropelength $\lambda_K = \lambda(\#K)$.

13.6 Bending energy spectra

It is interesting to compare groundstate magnetic energy spectra with the corresponding bending energy spectra obtained by considering bending energy in place of magnetic energy. Since magnetic relaxation is driven by the Lorentz force, that is mainly a curvature force, computation of the elastic energy due solely to curvature (bending energy) provides an interesting comparison. Bending energy is defined by

$$E_b = \frac{1}{2} \oint_{\mathcal{C}} K_b [c(s)]^2 ds, \tag{13.6.1}$$

where K_b is bending rigidity and $c(s)$ is local curvature. By normalizing this quantity with respect to the reference value $E_o = \pi K_b / R^* = K_b 2^{1/3} \pi^{5/3}$ of the tight torus, we have the normalized bending energy given by

$$\tilde{e} = \frac{E_b}{E_o} = \frac{\oint_{\mathcal{C}} [c(s)]^2 . ds}{2^{4/3} \pi^{5/3}}. \tag{13.6.2}$$

By using curvature data of tight knots obtained by RIDGERUNNER, we can easily plot the energy spectrum $\tilde{e} = \tilde{e}(\#K)$ according to increasing ropelength data. The corresponding energy spectra are shown in figure 13.4. Remarkably, and similarly to the magnetic

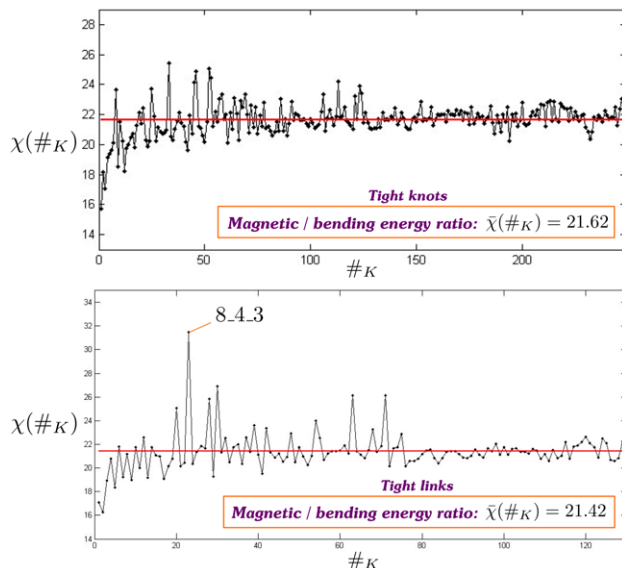


Fig. 13.5: Ratio of magnetic to bending energy $\chi = \tilde{m}/\tilde{e}$ of tight knots (top) and tight links (bottom) plotted against the knot/link number $\#_K$, given by the position of the knot/link K listed according to increasing value of ropelength $\lambda_K = \lambda(\#_K)$.

case, bending energy levels of knot and link types seem to follow an almost identical logarithmic law given by the best fit curve shown in the plots.

13.7 Magnetic energy versus bending energy

Let us compare the energy values by taking the ratio of magnetic to bending energy $\chi = \tilde{m}/\tilde{e}$ and plot for comparison $\chi = \chi(\#_K)$ according to increasing ropelength data. Results are presented in figure 13.5. As we see, with a few exceptions, ratios tend to level up around a constant value that for sufficiently large c_{\min} for tight knots is given by $\bar{\chi} = 21.62$ and for tight links is given by $\bar{\chi} = 21.42$. Thus, on average, for complex topologies we see that information on bending energy is proportional to magnetic energy. This is actually in good agreement with expectations: since magnetic relaxation is driven by the Lorentz force, which to a first approximation is a curvature force, it is not so surprising to discover that relaxed magnetic states are, on average, proportional to bending energy end-states of tight knots and links. Departure from average values is greater at lower c_{\min} , where, probably, the constraints imposed by the assumptions affect the most the results.

Let us now re-examine a common feature of the plots of figures 13.3-13.4. The curves dotted by circles results from a linear fit made over each c_{\min} -family, while

the continuous curve is the best-fit interpolation over all available data. To the first decimal digit, we find that best-fit interpolations follow an almost identical logarithmic law, given by

$$\tilde{m}(\#_K) = a \ln \#_K + b, \quad (13.7.1)$$

with $a = 4.5$, $b = 10.5$ for magnetic knots and $a = 4.5$, $b = 9.3$ for magnetic links, and similarly

$$\tilde{e}(\#_K) = a \ln \#_K + b, \quad (13.7.2)$$

with $a = 0.2$, $b = 0.6$ for elastic knots and $a = 0.2$, $b = 0.5$ for elastic links. These unexpected results are quite remarkable and call for some justification.

Ropelength is certainly an increasing function of topological complexity (given by c_{\min}), also because an increasing number of crossings implies an increasing minimal length necessary to tie a flux tube into a knot or a link. Results on ropelength bounds [4, 6, 8, 9] show that

$$O(c_{\min}^{3/4}) \leq \lambda_K \leq O(c_{\min} \ln^5 c_{\min}), \quad (13.7.3)$$

where $O(\cdot)$ denotes order of magnitude. From (13.5.2) we have that $\tilde{m}(\#_K) \propto [\lambda(\#_K)]^{4/3}$; by combining this with (13.7.2), we have

$$[\lambda(\#_K)]^{4/3} \propto a \ln \#_K + b. \quad (13.7.4)$$

Now, if we assume that the number of knots grows exponentially with c_{\min} (a plausible assumption), then $\#_K \sim C^{c_{\min}}$ for some constant C . Hence, by (13.7.4) we have $[\lambda(\#_K)]^{4/3} \propto c_{\min}$, or

$$\lambda(\#_K) \propto c_{\min}^{3/4}, \quad (13.7.5)$$

a result that, if not true in full generality, is certainly in good agreement with the lower estimate given by (13.7.3). Furthermore, let us set (for simplicity) $V = \Phi = 1$ in (13.3.5), and define

$$\overline{m}(c_{\min}) \equiv \frac{M_{\min}}{m_o} = \frac{1}{\pi} c_{\min}. \quad (13.7.6)$$

We can then relate (13.3.5) to (13.5.2), and write

$$\langle \tilde{m}(K) \rangle_{c_{\min}} \geq \overline{m}(c_{\min}) = \frac{1}{\pi} c_{\min}, \quad (13.7.7)$$

since for any given K $\tilde{m}(K)$ can be further decreased to its actual minimum by relaxing the constraints (i)-(iv) of Theorem 2. Similar considerations apply to $\tilde{e}(K)$. By writing (13.5.2) in terms of $\#_K$ and substituting this latter into the above equation, we have

$$\langle \lambda(\#_K) \rangle_{c_{\min}} \geq 2\pi^{1/4} c_{\min}^{3/4}, \quad (13.7.8)$$

that gives a new relation between ropelength, averaged over each c_{\min} -family, and c_{\min} . Note that the coefficient $2\pi^{1/4} \approx 2.66$ is independent of the knot family, and this result, in good agreement with (13.7.3), is still one of the best analytical results valid for any c_{\min} to date (see, for instance, [4]).

13.8 Conclusions

By using analytical results for the constrained minimum energy of magnetic knots obtained in [11], we have established a general functional relationship between minimum energy levels of knots and links and internal twist h , given by an $h^{4/3}$ -power law. In the case of standard flux tubes our result is in good agreement with an earlier result by [7] obtained by a scaling argument. By using ropelength data obtained by the RIDGERUNNER tightening algorithm developed by [1] we have computed the groundstate energy spectra of the first 250 prime knots and 130 prime links; we have shown that the two spectra follow an almost identical logarithmic law. We have then extracted data on curvature and by computing the bending energy we have compared magnetic and bending energy spectra, finding a remarkable proportionality between end-states. By assuming that the number of knot types grows exponentially with the topological crossing number c_{\min} , we have shown that this generic behavior can be justified by a general relationship between ropelength and crossing number, that is independent of the number of components (knots or links). Moreover, by considering ropelength averaged over a given knot family, we have established a new relation between this averaged ropelength and $c_{\min}^{3/4}$, valid for knots/links of *any* c_{\min} . However, as recent analytical work shows [9], these results cannot be considered fully general and further improvements are expected. In the context of magnetic relaxation, corrections are expected to come from finer realization of the analytical constraints (for instance, by allowing the cross-section to adapt to optimal shape) and from further improvements of the tightening procedure. In any case, our results demonstrate the great potential of magnetic energy methods to investigate and establish new relationships between energy contents and topological properties of complex systems. Moreover, by using curvature information of tight knots and links we can also estimate optimal properties of 3D-packing and global geometry. These results can find useful applications in many disparate fields, from the study of structural complexity of physical and biological filamentary systems [10, 18, 5], to applications in plasma physics and solar physics [15, 19]. They may also provide new insight into the ongoing search for fundamental aspects in the mass-energy relations of high-energy theoretical physics [3, 2].

Acknowledgment: R.L.R. wishes to express his gratitude to the Fonds National Suisse (FNS) for financial support.

Bibliography

- [1] Ashton, T., Cantarella, J., Piatek M. & Rawdon, E. (2011) Knot tightening by constrained gradient descent. *Experim. Math.* 20 57–90.

- [2] Buniy, R. V., Cantarella, J., Kephart, T. W. & Rawdon, E. J. (2014) Tight knot spectrum in QCD. *Phys. Rev. D* 89, 054513.
- [3] Buniy, R. V. & Kephart, T. W. (2005) Glueballs and the universal energy spectrum of tight knots and links. *Int. J. Mod. Phys. A* 20 1252–1259.
- [4] Buck, G. & Simon, J. (1999) Thickness and crossing number of knots. *Topol. Appl.* 91 245–257.
- [5] Buck, G. & Simon, J. (2012) The spectrum of filament entanglement complexity and an entanglement phase transition, *Proc. Roy. Soc. A* 468 4024–4040.
- [6] Cantarella, J., Kusner, R. B. & Sullivan, J. M. (2002) On the minimum ropelength of knots and links. *Invent Math* 150 257–286.
- [7] Chui, A. Y. K. & Moffatt, H. K. (1992) Minimum energy magnetic fields with toroidal topology. In *Topological Aspects of the Dynamics of Fluids and Plasmas*, (ed. H.K. Moffatt *et al.*), pp. 195–218. Kluwer Acad. Pubs., Dordrecht.
- [8] Diao, Y. (2003) The lower bounds of the lengths of thick knots. *J. Knot Theory Its Ram.* 12 1–16.
- [9] Diao, Y., Ernst, C., Por, A. & Ziegler, U. (2016) The ropelengths of knots are almost linear in terms of their crossing numbers. Preprint at arXiv: 0912.3282 (accessed on 20 April, 2018).
- [10] Kauffman, L. H., Editor (1995) *Knots and Applications*. Series of Knots and Everything 6. World Scientific, Singapore.
- [11] Maggioni, F. & Ricca, R. L. (2009) On the groundstate energy of tight knots. *Proc. R. Soc. A* 465 2761–2783.
- [12] Moffatt, H. K. (1985) Magnetostatic equilibria and analogous Euler flows of arbitrarily complex topology. Part I. Fundamentals. *J Fluid Mech* 159 359–378.
- [13] Moffatt, H. K. (1990) The energy spectrum of knots and links. *Nature* 347 367–369.
- [14] Moffatt, H. K. (2001) Some remarks on topological fluid mechanics. In *An Introduction to the Geometry and Topology of Fluid Flows*, (ed. R.L. Ricca), p. 3. Kluwer Acad. Pubs., Dordrecht.
- [15] Moffatt, H. K., Bajer, K. & Kimura, Y., Editors (2013) *Topological Fluid Dynamics: Theory and Applications*. Elsevier, Dordrecht.
- [16] Ricca, R. L. (2008) Topology bounds energy of knots and links. *Proc. R. Soc. A* 464 293–300.
- [17] Ricca, R. L., Editor (2009) *Lectures on Topological Fluid Mechanics*. Springer-Verlag, Heidelberg.
- [18] Ricca, R. L. (2009) Detecting structural complexity: from visiometrics to genomics and brain research. In *Mathknow* (ed. M. Emmer and A. Quarteroni), pp. 167–181. Springer-Verlag, Berlin.
- [19] Ricca, R. L. (2013) New energy and helicity lower bounds for knotted and braided magnetic fields. *Geophys. Astrophys. Fluid Dyn.* 107 385–402.
- [20] Ricca, R. L. & Maggioni, F. (2014) On the groundstate energy spectrum of magnetic knots and links. *J. Phys. A: Math. & Theor.* 47, 205501.
- [21] Rolfsen, D. (1976) *Knots and Links*. Publish or Perish, Berkeley.

- [22] Spivak, M. (1979) *A comprehensive introduction to differential geometry*. Vol. 1. Publish or Perish, Houston.
- [23] Stasiak, A., Katritch, V. & Kauffman, L. H. Editors, (1998) *Ideal Knots*. Series on Knots and Everything 19. World Scientific, Singapore.